Thermal expansion effects and heat conduction in granular materials

Watson L. Vargas and J. J. McCarthy*
Department of Chemical and Petroleum Engineering, University of Pittsburgh, Pittsburgh, Pennsylvania 15261, USA
(Received 25 April 2007; revised manuscript received 16 August 2007; published 16 October 2007)

In this paper, we report results and analysis on a simulation study of the effects of thermal expansion in granular systems. We show that these effects impact the force distribution inside a two-dimensional system of disks that are subject to thermal heating under two different boundary conditions. A significant increase in the average force is observed for steel particles confined within a box with fixed walls at temperature rises of 50 °C and 100 °C, respectively. As previously noted in the literature, thermal expansion also induces compaction. The results show that a systematic and controllable increase in granular packing can be induced by simply raising and then lowering the temperature, without the input of mechanical energy in agreement with previous experimental observations. We find that the evolution of the packing fraction is well described by a fractional relaxation model, which follows the Mittag-Leffler law.

DOI: 10.1103/PhysRevE.76.041301 PACS number(s): 45.70.Cc, 83.80.Fg, 65.40.De

I. INTRODUCTION

Under the effect of external forces, noncohesive granular materials develop a highly nonhomogeneous network of stressed particles, which carries most of the applied force, while some particles within the bed are effectively isolated from their neighbors and carry no load at all. An example of this network is shown in Fig. 1. Because the interparticle forces and their distribution determine the bulk properties of a granular system, this behavior has very important consequences in transport phenomena such as heat transfer [1,2], sound propagation [3], and electrical conduction [4–7].

Experimental work under different settings has revealed the sensitivity of granular materials to small perturbations of the grains. Liu and Nagel [3,8] reported on the effect of thermal expansion on sound propagation in granular media. Their results revealed that the thermal expansion of a single glass bead of the order of ≃3000 Å can generate a 25% drop in sound propagation. Yet another recent experimental study that shows the importance of thermal expansion in granular media is the study by Chen *et al.* [9] on the consolidation of grains by thermal cycling. Chen *et al.* showed that it is possible to increase the packing fraction of a granular bed by a systematic and controlled cycling of the temperature. Changes in the packing fraction up to 1% were observed in beds of glass particles contained in a plastic cylinder with a cycling temperature difference of ≃120 °C.

Due to the nature of the distribution of contacts—and forces—in a granular pack (see Fig. 1), the electrical and thermal contacts can be widely distributed. Given the cross-property connection between thermal or electrical conductivity and its dependence on the geometry of the contact [10,11], it is expected that thermal expansion will play a significant role on the conduction both of thermal and electrical energy in granular packs of particles.

In this paper, we report results and analyses on a simulation study on the effects of thermal expansion on the force distribution in two-dimensional granular packs under compression, as well as compaction by thermal cycling in a three-dimensional (3D) packed bed using thermal particle dynamics (TPD)—a modified discrete element simulation introduced by the authors [1]. Here we show that thermal expansion of the grains in a granular pack can induce significant changes in the microstructure, without the input of mechanical energy, even for mild temperature differences. This thermal effect may have important practical implications for the handling and storage of granular materials.

II. THERMAL PARTICLE DYNAMICS

The TPD simulation technique is based upon a traditional particle dynamics (PD) technique (often referred to as the discrete or distinct element method [12]) so that every particle is tracked individually to determine trajectories, velocities, forces, and temperatures. This allows the determination of both mechanical and transport properties of granular systems under static and/or dynamic conditions. Again, the particle trajectories are obtained via the explicit solution of Newton's equations of motion for every particle [12] and the forces on the particles are determined from contact mechanics considerations [13]. The equations that describe the particle motion are as follows:

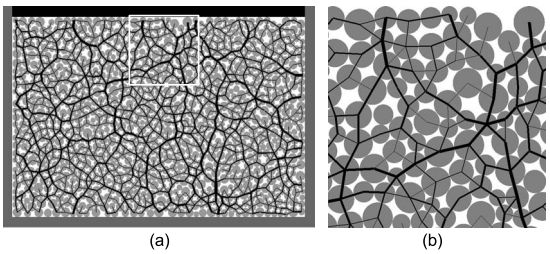

FIG. 1. Stress chains in a particle bed under external loading. (a) The lines joining the centers of particles in contact represent the force network and have thickness proportional to the contact force. (b) Note that the heterogeneities in the stress chains are evident even in the rescaled region.

*Corresponding author; mccarthy@granular.che.pitt.edu

Linear motion:

$$m_i \frac{d\mathbf{v}_i}{dt} = \mathbf{F}_b + \mathbf{F}_n + \mathbf{F}_t. \tag{1}$$

Angular motion:

$$I_i \frac{d\boldsymbol{\omega}_i}{dt} = \mathbf{F}_t \times \mathbf{R}_i, \tag{2}$$

where m_i is the mass of particle i, $\mathbf{v}$ is the velocity, $\mathbf{F}_b$ represents any relevant body forces, $\mathbf{F}_n$ is the force normal to the contact plane, $\mathbf{F}_t$ is the force tangent to the contact plane, I is the moment of inertia, $\boldsymbol{\omega}$ is the angular velocity, $\mathbf{R}$ denotes the vector connecting the particle centers, and t is time. Note that bold text denotes vector quantities. Computationally, the deformation at a particle-particle contact point is realized as a small "overlap" of the particles.

The key feature of TPD is that by incorporating contact conductance theories many simultaneous two-body interactions may be used to model heat transfer in a system composed of many particles. In analogy with PD, this description requires that the time step be chosen such that any disturbance (in this case a change in a particle's temperature) does not propagate further than that particle's immediate neighbors within one time step. The details of the simulation technique are identical to those used in Vargas and McCarthy [1,2] and the reader is referred to those publications for more details, as only a quick review is included here.

Contact conductance refers to the ability of two touching materials to transmit heat across their mutual interface and is the key ingredient added to PD in order to form TPD. The most basic problem in contact conductance is that between two smooth, elastic particles under vacuum with a small, but finite area of contact (as assumed in this study). In this problem, the "resistance" to heat transfer is assumed to be solely due to the constriction of heat flow lines such that the heat flux across the contact area Q between the two particles is

$$Q_{ij} = H_c(T_j - T_i), \tag{3}$$

where $\Delta T_{ij} = T_i - T_j$ is the temperature difference between the midplanes of the spheres, and H_c is the contact conductance. Approximate analytical solutions have been proposed independently by Yovanovich [14], Holm [15], and Batchelor and O'Brien [16]. The contact conductance between spheres can be approximated by $H_c = 2k_s a$. The contact radius a is obtained from Hertz's elastic contact theory, such that the contact conductance is given by

$$H_c = 2k_s \left[\frac{3F_n r^*}{4E^*} \right]^{1/3}, \tag{4}$$

where E^* is the effective Young's modulus for the two particles in contact, and r^* is the effective radius. As indicated by Eq. (4), H_c is not a constant value but changes at every time step depending on the instantaneous normal force between the particles.

Incorporating the concept of contact conductance into a PD model—in order to formulate the TPD method—can be accomplished by summing the pairwise thermal interactions so that the net heat input to particle i is given as

$$Q_i = \sum_{j=1}^{N} Q_{ij} \tag{5}$$

so that the evolution of the temperature of particle i may be given as

$$\frac{dT_i}{dt} = \frac{Q_i}{\rho_i c_i V_i}, \tag{6}$$

where $\rho_i c_i V_i$ is the particle's "thermal capacity." Note that this approach requires two caveats. First, that the Biot number for the particle heating problem is very small. That is, that the internal thermal transport is much faster than the external thermal transport. Second, that thermal transients are small enough that using the quasisteady heat flow given by Eq. (3) may be used—incorporating a contact "capacitance" is possible to alleviate this caveat [17] but has not proved necessary over the time scales examined in our current topics of research.

To take into account the effect of the thermal expansion the change in the radius of the particles due to expansion is incorporated into the simulation as

$$r = r_0 + \beta \Delta T, \tag{7}$$

where r_0 is the initial radius of the particles at the reference temperature, β is the thermal expansion coefficient of the solid particle material, r is the current radius, and ΔT is the temperature rise relative to the reference temperature. A similar approach has been previously applied by Lu *et al.* [18].

As the purpose of this work is to elucidate the importance of thermal expansion of the grains on the heat transfer process, the main heat transfer mechanism in the systems considered here is that of conduction between particles and between particles and walls. Since the temperatures concerned in this study are relatively low, radiant heat transfer is neglected. No explicit effort has been made to incorporate the effect of temperature on properties such as Young modulus or yield stress. It is assumed that over the mild temperature changes used in this work, their values remain constant. Extensions of TPD to include the effect of stagnant interstitial fluids (applicable at small Rayleigh numbers) are straightforward and have been detailed elsewhere [19]. Similar approaches have been developed for flowing gas-solid systems [20,21].

III. RESULTS AND DISCUSSION

A. Heat conduction with thermal expansion

Visualization of two-dimensional granular systems applying stress-induced birefringence [22] as well as results coming from numerical studies demonstrate that forces within granular media follow preferred paths, the so-called stress chains or force chains network [23]. The effect of stress chains on heat conduction in a granular bed was previously explored by Vargas and McCarthy [1,2], where it was found that heat flow along stress chains is significantly enhanced along their axis, but hampered if running perpendicular to those same stress chains. In an effort to evaluate the stress levels to which particles are subjected due to thermal cy-

TABLE I. Parameters used in the simulation.

Parameter	Glass	Steel
Density (kg/m^3)	2500	7900
Poisson ratio	0.23	0.29
Young's modulus (Gpa)	68.9	193
Conductivity (W/m K)	1.1	14.7
Heat capacity (J/kg K)	800	477
Coefficient of thermal expansion (1/K)	9.0×10^{-6}	17.5×10^{-6}
Coefficient of friction	0.3	0.3

cling, the dynamics of stress chains within a granular bed, undergoing thermal expansion, are computationally studied here.

The simulation consists of a polydisperse system of perfectly smooth noncohesive disks forming a random two-dimensional packed bed (one-particle deep), compressed by a wall of known weight. All material properties are taken directly from the literature and consist solely of the mechanical properties of the applicable solid (see Table I). A typical initial condition for simulation is obtained by perturbing a hexagonal lattice and allowing the particles to settle under gravity. Particles settle onto a planar bottom wall under the action of gravity and a consolidating wall loaded by a constant weight. A load equivalent to 1000 N, which corresponds to roughly 800 times the weight of the particle bed, was used in all cases, unless stated otherwise. This was done in order to reduce the impact of the particles' weight on the stress distribution.

The thermal simulation proceeds as follows. An initially isothermal bed of particles under a uniaxial load, in which the two side walls are insulated and the top wall is at a low constant temperature, is subject to a step change in temperature at the bottom wall. The thermal and mechanical response of the bed of granular material is followed in time until the system reaches steady state; that is, until the $Q_{In}=Q_{Out}$.

Figure 2 shows a stress field superimposed on the temperature field for two different conditions of the top wall. The black lines represent particle contacts which experience forces above the average and have thickness scaled by their magnitude. Figure 2(a) illustrates a situation in which the top wall has been kept fixed during the heating process (i.e., a constant volume boundary condition). The temperature field shows that the propagation of heat is highly nonuniform and localized around highly stressed chains of particles. Figure 2(b) illustrates the case when the top wall is allowed to move freely as the bed is heated from the bottom (i.e., a constant stress boundary condition). Notice that the temperature is slightly more uniform when compared to Fig. 2(a). Thermal expansion of the particles, coupled with local rearrangement of the bed provides a simple hypothetical explanation (tested below) of this result.

A simple way to characterize the uniformity of the temperature field is a contoured temperature field of the beds as illustrated in Fig. 3. The results in Fig. 3(b) indicate a more uniform distribution of the temperature in the case of a bed

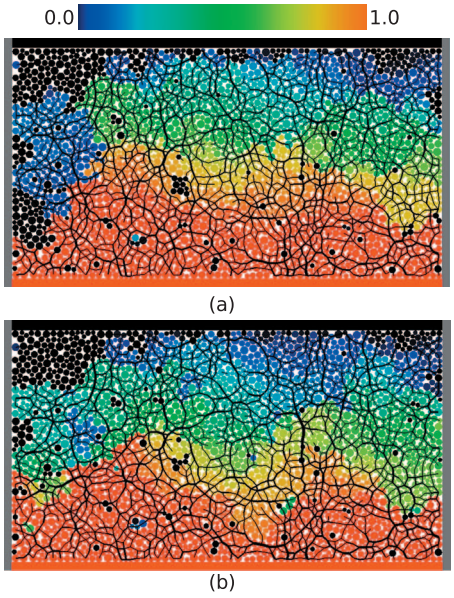

FIG. 2. (Color) Temperature-stress fields at steady state. (a) Bed with a fixed top wall. (b) Bed with a top freely moving wall. The black lines represent particle contacts, which experience forces above the average with thickness proportional to the contact force, while colors represent dimensionless temperatures (red corresponds to hot).

with moving wall as previously indicated qualitatively in Fig. 2. This corresponds with local temperature gradients being smoothed.

Computational experiments on granular material provide a unique opportunity to measure quantities that are experimentally difficult to measure in physical systems. A common way to analyze the distribution of forces in granular materials is to determine the probability distribution function $P(f)$ of interparticle normal-force magnitudes $f=F/\langle F\rangle$ between neighboring particles, where $\langle . \rangle$ indicates the average over all the grains in the bed. Several features are common to force distribution in granular media. The probability density function (PDF) decays in an exponential manner for forces above the average (i.e., $f>1$), and has a peak and/or a plateau around the mean force $f\approx1$. Both experiments [23] and simulations [24–26] have shown that "force chains" and $P(f)$ are different for shearing than for uniaxial compression and are history dependent. We use the contact forces obtained from the computational experiments to investigate the effect of thermal expansion on $P(f)$.

The probability distribution function of normal forces for various times, i.e., 0, 30, 120, and 240 s, at a constant temperature difference of 100 °C and 50 °C for a 2D bed with fixed and moving walls, are shown in Fig. 4. The times used in Fig. 4 illustrate different stages in the dynamics, i.e., initial condition, initial stage of heating, late stage of heating, and steady state. The force has been normalized by the average normal force at each specific time. The results show that regardless of the boundary conditions imposed or the effects of thermal expansion, the probability distribution function does not change when normalized with its own mean value.

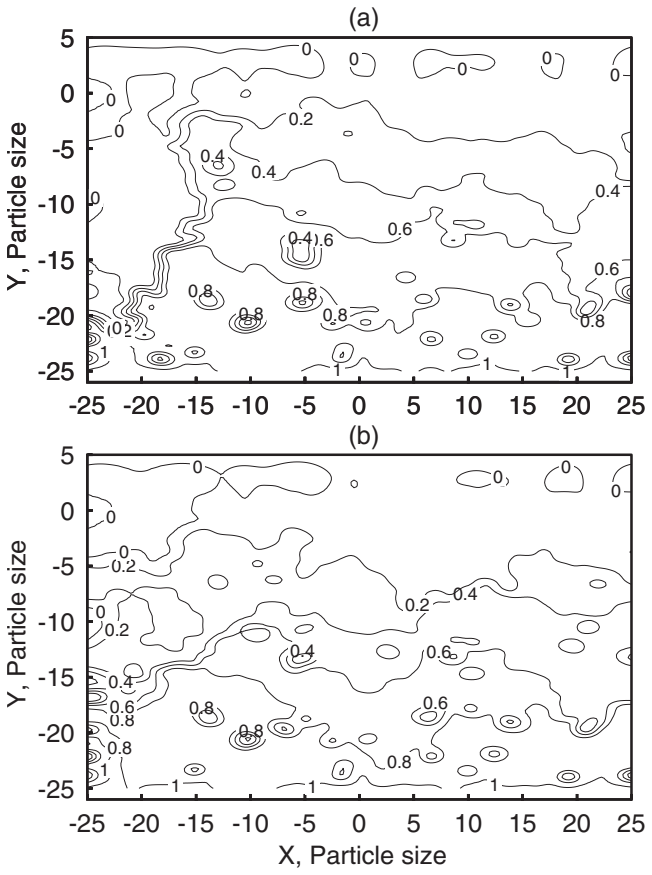

FIG. 3. Contour plot for two-dimensional beds at a temperature difference $\Delta T = 100$ °C. (a) Fixed wall, constant volume boundary condition. (b) Moving wall, constant stress boundary condition.

To better understand the qualitative change in behavior between the system with a fixed wall and that with a freely moving wall, as a function of time, we determine the evolution of average force $\langle F \rangle$ as the bed is heated from an isothermal initial condition ($T=0$). Figures 5(a) and 5(b) show the average force for the bed with a fixed wall and the freely moving wall, respectively. For the fixed wall system [Fig. 5(a)] the results show a continuous increase in the average force with time, which reaches a saturation point once the bed is at steady state. Both temperature differences reveal the same trend, although the saturation values are different, as expected.

From a practical perspective, this result implies that when dealing with packing of grains subjected to heating, a compromise has to be made: beds under fixed confinement and with high initial densities might be easier to implement physically, but at the same time the stresses induced by thermal expansion are expected to be much higher and may be detrimental to the integrity of the particles. Thermally induced microcracking of the particles can severely damage a packed bed reactor or any other device that uses particles as a means to promote reaction or heat transfer [18,27].

In contrast to the fixed wall system, the bed with a freely moving wall [Fig. 5(b)], shows a constant average force with time for both temperature differences of 50 °C and 100 °C, respectively. A plot of the time evolution of the packing fraction (Fig. 6) reveals that both systems follow the same trend, both reaching approximately the same steady-state density. The results in Fig. 6 suggest a slow relaxation process, representative of the collective rearrangement of many grains. These results are in agreement with results by Brujic *et al.* [28] on the relaxation of granular materials at infinitesimal strain perturbations.

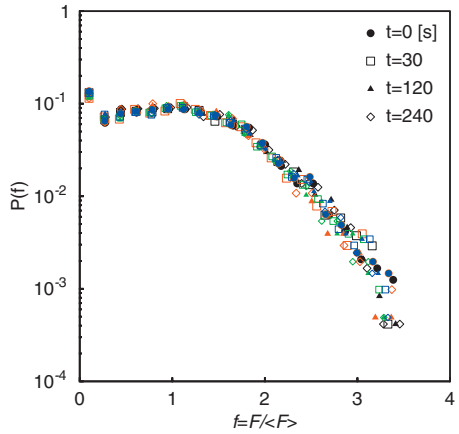

FIG. 4. (Color) Probability distributions of the normal forces for compressed beds with a fixed and moving wall under the effect of thermal expansion. The forces have been normalized by the individual systems' average force at each specific time. Black symbols: moving wall at a temperature difference of 100 °C. Red symbols: fixed wall at a temperature difference of 100 °C. Green symbols: fixed wall at a temperature difference of 50 °C. Blue symbols: moving wall at a temperature difference of 50 °C.

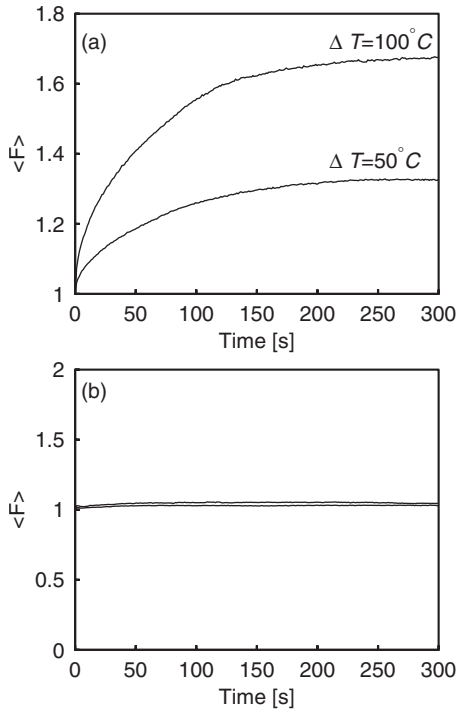

FIG. 5. Evolution of the average normal force. (a) System with fixed wall. (b) System with moving wall. The force has been normalized with the average force of the cold ($T=0$) isothermal bed at $t=0$.

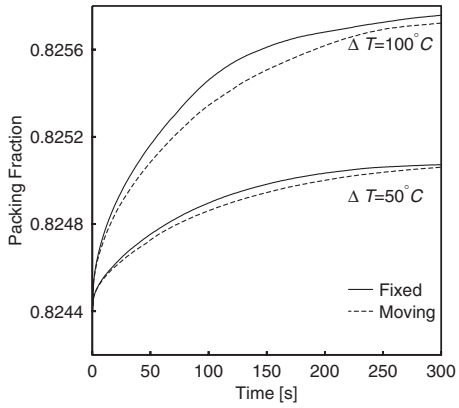

FIG. 6. Time evolution of the packing fraction for the systems with fixed and moving walls. The slightly higher densification in the fixed wall system is traced back to thermal expansion of the particles and a small difference in the wall height, which corresponds to $26.83d_p$ for the fixed wall and $26.86d_p$ at steady state for the freely moving wall at $\Delta T=100$ °C. The same applies at $\Delta T=50$ °C.

The dynamics induced by thermal expansion generates different effects. On one hand it alters the average force in the system as illustrated above. It also generates changes in the structure of the contacts network [23]. In order to investigate these changes, we study the evolution of average parameters such as coordination number $\langle Z\rangle$ and average temperature of the bed $\langle T\rangle$. The bed with fixed walls [Fig. 7(a)] shows an increase in the average coordination number from an initial value of 3.58 to 3.67 at steady state. The bed with a freely moving wall (dashed line) maintains a value that oscillates around the average of 3.58. The time required to reach a steady average value in the average temperature is, however, different for the two systems [Fig. 7(b)], with the fixed wall system showing a slightly higher initial rate, and reaching the steady-state value at an earlier time.

Figure 8 illustrates the variation of the average force with mean radius of the particles for the two boundary conditions used in this study. For particles that follow a Hertzian contact mechanics, $F\propto\delta^{3/2}$, where δ is the "overlap" of the undeformed particles. If the bed were to expand with no microstructural rearrangements, one would expect that changes in r would proportionately change δ. Therefore, a plot of $\langle F\rangle$ vs $\langle r\rangle^{3/2}$ should be linear in the case of minimal rearrangement. For the fixed wall system [Fig. 8(a)] the results show almost a perfect line which, combined with the results of Fig. 7(a), seems to confirm microstructural continuity. The system with a freely moving wall, however, shows a constant value in the average force with increasing mean radius. In the later case the increase in radius is compensated by particle rearrangement as well as bed expansion in order to maintain a constant value in the average force.

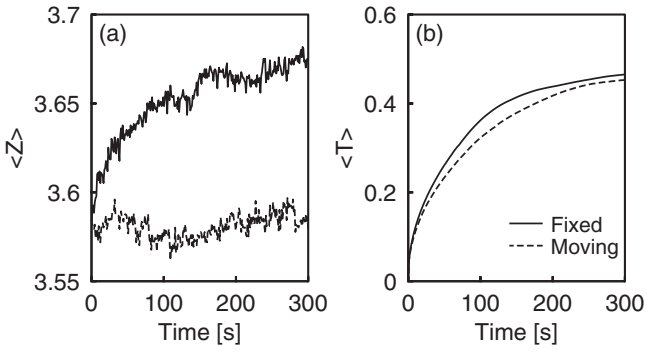

FIG. 7. Variation in average properties for the fixed wall (continuous line) and moving wall (dashed line) systems. The temperature difference for both systems is $\Delta T=100$ °C. (a) Mean coordination number. (b) Mean temperature of the bed.

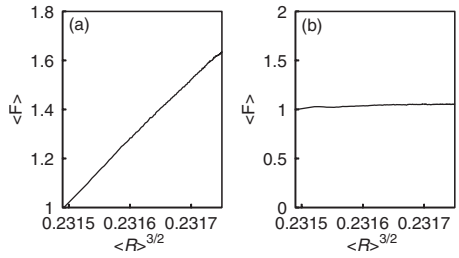

FIG. 8. Variation of the average force with particle radius. (a) System with fixed wall. (b) System with moving wall.

The results in this section reflect the extreme sensitivity of granular materials to perturbations. Even a change of the order of $\simeq 1.0-5.0$ μm in the particle radius generates measurable macroscopic effects. The numerical experiments show that although both systems reach similar macroscopic steady-state values for the density and temperature this does not prevent the existence of local fluctuations, which are reflected in the fact that the temperature fields look qualitatively and quantitatively different as illustrated in Fig. 2.

B. Compaction by thermal cycling

A significant number of industrial products are processed, transported, and stocked in a granular state. The packing fraction of those granular materials becomes therefore a relevant parameter for a broad range of applications. From a practical perspective, the best way to reduce the costs for the manipulation of such granular materials is to increase the packing fraction. This has traditionally been achieved by tapping or vibrating the vessel containing the grains. A recent study by Chen *et al.* [9] has demonstrated that the same result can also be accomplished by thermal cycling.

The packing fraction of a granular material is defined as the fraction of sample volume that is filled by grains rather than by empty space, and for a 3D system typically varies between 57% and 64% for randomly arranged, spherical particles and even more widely for other particle shapes. Several studies have reported on compaction of granular materials by vibration or tapping, which induce rearrangements that allow the grains to settle [29]. Studies on the grain dynamics induced by thermal cycling either experimentally [9] or computationally are scarce.

When a granular material is heated, both container and grains undergo thermal expansion. This generates settling be-

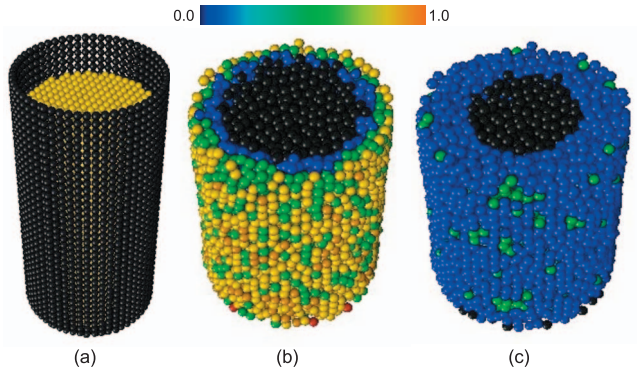

FIG. 9. (Color) Packing by thermal cycling using TPD. (a) Initial condition. Snapshot of the bed during the (b) heating cycle, and (c) cooling cycle. In (b) and (c), the walls of the vessel have been removed to facilitate the visualization.

cause of the relatively fragile nature of the microstructure, according to Chen *et al.* [9]. This seem to be particularly significant when the grains and container are made of different materials with different thermal expansion. The settling is not reversible upon cooling to ambient temperature, as shown recently in Ref. [9]. Here we examine the packing fraction for glass spheres contained in a vertical cylinder in response to repeated thermal cycling from a reference temperature, much in the same way as the experiments conducted by Chen *et al.* [9].

The simulation consists of a narrowly polydisperse system of perfectly smooth noncohesive spheres of diameter d_p and mass m forming a random three-dimensional packed bed, bounded by a rough wall and an open top [see Fig. 9(a)]. All material properties are taken directly from the literature and consist solely of the mechanical properties of the solid (see Table I). A typical initial condition for simulation is obtained by perturbing a 3D lattice and allowing the particles to settle. Particles settle onto a rough bottom wall under the action of gravity (Fig. 9).

The thermal simulation proceeds as follows. The initially low temperature isothermal bed of particles, is subject to a step change in temperature at the bottom and side walls, and the thermal and mechanical response of the bed of granular material is followed in time until the system reaches steady state. At this point the system is given another step change in temperature and is allowed to cool down until reaching steady state. This process is repeated as many cycles as required [Figs. 9(b) and 9(c)]. The results of this exercise on packing fraction are shown in Fig. 10.

We start with an initial solid fraction of 59.0%, which is typical of spheres poured into a container and not compacted. The results indicate that there is a clear increase in packing even for a single cycle. This observation is consistent with the experimental data reported by Chen *et al.* [9]. In Fig. 10 the packing fraction continues to increase over multiple thermal cycles and seems to reach a plateau at a high number of cycles. This behavior is similar for the three temperature rises applied in this study. Chen *et al.* argued that the primary cause of the changes in packing fraction is the difference between the thermal expansion of the grains and the container. Our simulations—which do not account for

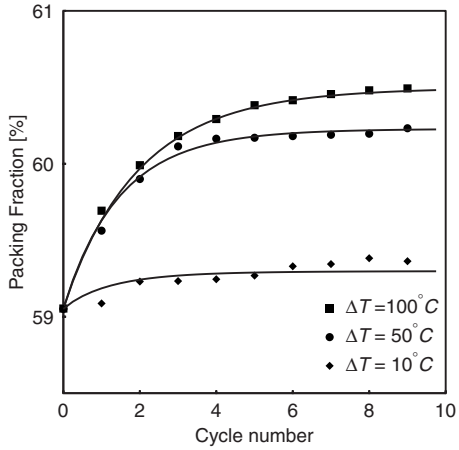

FIG. 10. Change in packing fraction with thermal cycling for a temperature difference of 10 °C, 50 °C, and 100 °C between the cooling and heating cycle. The solid lines are the Mittag-Leffler fits of Eq. (8), with parameters α and τ given in Table II.

thermal expansion of the wall—show similar trends although with smaller changes in packing. These results might suggest that while the expansion of the walls may increase the degree of compaction attained, it is not necessary. Instead, expansion or contraction of only the particles is enough to achieve bed compaction.

Several empirical and theoretical models have been proposed in the literature to describe density relaxation, primarily in vibration and tapping experiments [28,30–34]. The compaction dynamics observed in Fig. 10 is well described by the fractional Mittag-Leffler law for relaxation [29,35]

$$\rho(t) = \rho_\infty - \Delta\rho E_\alpha\left[-\left(\frac{t}{\tau}\right)^\alpha\right], \quad \Delta\rho = \rho_\infty - \rho_0, \quad 0 < \alpha < 1, \tag{8}$$

where, ρ_0 is the initial packing fraction and ρ_∞ is the packing fraction at steady state. E_α denotes the ordinary Mittag-Leffler function of order α, with series expansion [35,36]

$$E_\alpha\left[-\left(\frac{t}{\tau}\right)^\alpha\right] = \sum_{n=0}^{\infty} \frac{[-(t/\tau)^\alpha]^n}{\Gamma(1+\alpha n)}, \quad \alpha > 0. \tag{9}$$

The parameters α and τ determine the rate of compaction on the current time scale and the characteristic time of the densification process, respectively. τ and α are treated here as fitting parameters.

Note that the fitting function in Eq. (8) is a solution of the fractional relaxation equation [29,35]

TABLE II. Estimated parameters for the Mittag-Leffler law.

ΔT	α	τ
10	0.95	1.3
50	0.98	1.5
100	0.98	2.0

$$\tau_\alpha^\alpha \, {}_0D_t^\alpha \Delta\rho(t) = -\Delta\rho(t), \tag{10}$$

where $\Delta\rho = \rho_\infty - \rho(t)$. Equation (10) is solved subject to the initial conditions

$$\Delta\rho(0) = \rho_\infty - \rho_0, \tag{11a}$$

$$\Delta'\rho(0) = 0. \tag{11b}$$

The operator ${}_0D_t^\alpha$ in Eq. (10) is the so-called Caputo fractional derivative, defined as [36]

$${}_0D_t^\alpha f(t) = \frac{1}{\Gamma(n-\alpha)} \int_0^t (t-\tau)^{n-\alpha-1} f^{(n)}(\tau) d\tau,$$

$$(n-1) < \alpha \leq n. \tag{12}$$

As indicated by Eq. (12), for $n=1$, the fractional operator introduces a power-law kernel $\phi(t) \propto t^{-\alpha}$ [29]. The convolution integral therefore involves a decaying memory, so that the current packing fraction $\rho(t)$ depends on its previous history. A comprehensive solution to Eq. (10) has been provided by Hilfer [35] in terms of the Riemann-Liouville operator for fractional derivatives.

The Mittag-Leffler law model has been previously applied to fit simulation data on the compaction of granular materials under vertical taping [29] and relaxation of glassy systems [37]. This model is very closely related to the stretched exponential model $\rho(t) = \rho_\infty - (\rho_\infty - \rho_0)\exp[-(t/\tau)^\beta]$ used by Richard *et al.* [34] on slow relaxation and compaction of granular media and which Barker and Mehta [30] pointed out, also fit their experimental data on compaction. Note that the Mittag-Leffler function is related to the exponential function when $\alpha=1$, such that

$$E_1 = \sum_{n=0}^{\infty} \frac{[-(t/\tau)^\beta]^n}{\Gamma(1+n)} = \exp\left[-\left(\frac{t}{\tau}\right)^\beta\right], \tag{13}$$

and therefore, the stretched exponential is but a particular solution of the fractional relaxation model in Eq. (8).

As indicated by Richard *et al.* [34], granular compaction has a glassy behavior such that memory effects are important; the evolution of the packing fraction depends not only on the initial condition but also on its previous history. The model in Eq. (8) is well suited to this purpose since it intrinsically incorporates the memory effects. The continuous lines in Fig. 10 which represent the solution to the Mittag-Leffler model in Eq. (8), fit the data reasonably well.

It is interesting to note that Eq. (8) has been shown to describe the relaxation of granular materials under very different modes of external excitation; that is, vibration [30], tapping [29], and now thermal cycling (as shown by the results in Fig. 10). This suggests a connection between these relaxation processes and fractional dynamics despite different modes of perturbation. Fractional dynamics takes place in systems which are characterized by multiple trapping events—the caging of granular particles during thermal cycling being but one example—which create a random distribution of waiting times for the motion of individual particles to take place [38]. As the packing fraction increases, the time that grains spend in a cage becomes longer and longer until reaching a fixed position [29]. Mittag-Leffler responses are therefore expected in systems that exhibit this kind of behavior.

IV. PERSPECTIVE

Heat conduction in granular media with thermal expansion shows how elementary perturbations might have important consequences in transport phenomena. Nonlinearity is particularly important in unconsolidated or mildly consolidated media because the structure of the grain packing is determined by the fragile contacts between the grains. Thus even small vibrations or thermal expansions can cause the structure to evolve with time. This sensitivity tends to disappear when the media is subjected to a strong external load. We have demonstrated that TPD simulations of granular packings with thermal expansion offer insight into the behavior of granular media under uniaxial compression. The results indicate that even mild temperature differences can generate increases in the average contact forces, as well as structural rearrangements. Such changes may lead to detrimental consequences to the integrity of the particles.

A comparison of our simulations results on thermal packing with the experimental observations in Ref. [9] showed good agreement, although the experimental and computational systems present slightly different boundary conditions. A fractional relaxation model based on the well known Mittag-Leffler law has been found to provide the best fit to the results on compaction by thermal cycling. This generic law describes the relaxation of granular media under very different modes of external excitation.

ACKNOWLEDGMENTS

The authors would like to acknowledge the support of the Chemical and Transport Systems Division of the National Science Foundation (Grant No. 0331352).

[1] W. L. Vargas and J. J. McCarthy, AIChE J. **47**, 1052 (2001).
[2] W. L. Vargas and J. J. McCarthy, Chem. Eng. Sci. **57**, 3119 (2002).
[3] C.-H. Liu and S. R. Nagel, J. Phys.: Condens. Matter **6**, A433 (1994).
[4] D. Bonamy, L. Laurent, P. Claudin, J.-P. Bouchaud, and F. Daviaud, Europhys. Lett. **51**, 614 (2000).
[5] E. Falcon, B. Castaing, and M. Creyssels, Eur. Phys. J. B **38**, 475 (2004).
[6] S. Dorbolo, A. Ausloos, and N. Vandewalle, Appl. Phys. Lett. **81**, 936 (2002).
[7] M. Ghadiri, C. M. Martin, P. Arteaga, U. Tüzun, and B. Form-

isani, Chem. Eng. Sci. **61**, 2290 (2006).
[8] C.-H. Liu, Phys. Rev. B **50**, 782 (1994).
[9] K. Chen, J. Cole, C. Conger, J. Draskovic, M. Lohr, K. Klein, T. Scheidemantel, and P. Schiffer, Nature (London) **442**, 257 (2006).
[10] I. Sevostianov and M. Kachanov, Proc. R. Soc. London, Ser. A **460**, 1529 (2004).
[11] I. Sevostianov, M. Bogarapu, and P. Tabakov, Int. J. Fract. **118**, 77 (2002).
[12] P. A. Cundall and O. D. L. Strack, Geotechnique **29**, 47 (1979).
[13] K. L. Johnson, *Contact Mechanics* (Cambridge University Press, Cambridge, 1987).
[14] M. M. Yovanovich, J. Spacecr. Rockets **4**, 119 (1967).
[15] R. Holm, *Electrical Contacts: Theory and Application* (Springer-Verlag, New York, 1967).
[16] F. G. K. Batchelor and R. W. O'Brien, Proc. R. Soc. London, Ser. A **355**, 313 (1977).
[17] W. M. Siu and S. H.-K. Lee, Comput. Mech. **25**, 59 (2000).
[18] Z. Lu, M. Abdou, and A. Ying, J. Nucl. Mater. **299**, 101 (2001).
[19] W. L. Vargas and J. J. McCarthy, Int. J. Heat Mass Transfer **45**, 4847 (2002).
[20] Y. Shimizu, Powder Technol. **165**, 140 (2006).
[21] B. Chaudhuri, F. J. Muzzio, and M. S. Tomassone, Chem. Eng. Sci. **61**, 6348 (2006).
[22] G. W. Baxter, in *Powders and Grains 97*, edited by R. P. Behringer and J. T. Jenkins (Balkema, Rotterdam, 1997), pp. 223–226.
[23] T. S. Majmudar and R. P. Behringer, Nature (London) **435**, 1079 (2005).
[24] S. G. Bardenhagen, J. U. Brackbill, and D. L. Sulsky, Phys. Rev. E **62**, 3882 (2000).
[25] E. Aharonov and D. Sparks, Phys. Rev. E **65**, 051302 (2002).
[26] W. L. Vargas, J. C. Murcia, L. E. Palacio, and D. M. Dominguez, Phys. Rev. E **68**, 021302 (2003).
[27] A. Abou-Sena, A. Ying, and M. Abdou, Fusion Sci. Technol. **44**, 81 (2003).
[28] J. Brujic, P. Wang, C. Song, D. L. Johnson, O. Sindt, and H. A. Makse, Phys. Rev. Lett. **95**, 128001 (2005).
[29] D. Arsenovic, S. B. Vrhovac, Z. M. Jaksic, L. Budinski-Petkovic, and A. Belic, Phys. Rev. E **74**, 061302 (2006).
[30] G. C. Barker and A. Mehta, Phys. Rev. E **47**, 184 (1993).
[31] J. B. Knight, C. G. Fandrich, C. N. Lau, H. M. Jaeger, and S. R. Nagel, Phys. Rev. E **51**, 3957 (1995).
[32] J. J. Brey and A. Prados, J. Phys.: Condens. Matter **13**, 1 (2001).
[33] G. Lumay and N. Vandewalle, Phys. Rev. E **74**, 021301 (2006).
[34] P. Richard, M. Nicodemi, R. Delannay, P. Ribiere, and D. Bideau, Nat. Mater. **4**, 121 (2005).
[35] R. Hilfer, Fractals **11**, 251 (2003).
[36] F. Mainardi and R. Gorenflo, J. Comput. Appl. Math. **118**, 283 (2000).
[37] R. Hilfer, Phys. Rev. E **65**, 061510 (2002).
[38] R. Metzler and J. Klafter, J. Non-Cryst. Solids **305**, 81 (2002).